Journal of Proteomics 175 (2018) 144–155

Contents lists available at ScienceDirect

Journal of Proteomics

journal homepage: www.elsevier.com/locate/jprot

Novel identified aluminum hydroxide-induced pathways prove monocyte activation and pro-inflammatory preparedness☆

Sietske Kooijman[a,b], Jolanda Brummelman[c,1], Cécile A.C.M. van Els[c], Fabio Marino[b,d,2], Albert J.R. Heck[b,d], Geert P.M. Mommen[a,3], Bernard Metz[a], Gideon F.A. Kersten[a,f], Jeroen L.A. Pennings[e], Hugo D. Meiring[a,*]

[a] Intravacc, Bilthoven, The Netherlands
[b] Biomolecular Mass Spectrometry and Proteomics, Bijvoet Center for Biomolecular Research and Utrecht Institute for Pharmaceutical Sciences, Science Faculty, Utrecht University, The Netherlands
[c] Centre for Infectious Disease Control, National Institute for Public Health and the Environment, Bilthoven, The Netherlands
[d] Netherlands Proteomics Centre, Utrecht, The Netherlands
[e] Centre for Health Protection, National Institute for Public Health and the Environment, Bilthoven, The Netherlands
[f] Leiden Academic Centre for Drug Research, Leiden University, Leiden, The Netherlands

ARTICLE INFO

Keywords:
Quantitative proteomics
Aluminum hydroxide
Innate immunity
Antigen presentation
Systems-based approach
Human vaccine adjuvant

ABSTRACT

Aluminum-based adjuvants are the most widely used adjuvants in human vaccines. A comprehensive understanding of the mechanism of action of aluminum adjuvants at the molecular level, however, is still elusive. Here, we unravel the effects of aluminum hydroxide $Al(OH)_3$ by a systems-wide analysis of the $Al(OH)_3$-induced monocyte response. Cell response analysis by cytokine release was combined with (targeted) transcriptome and full proteome analysis. Results from this comprehensive study revealed two novel pathways to become activated upon monocyte stimulation with $Al(OH)_3$: the first pathway was IFNβ signaling possibly induced by DAMP sensing pathways like TLR or NOD1 activation, and second the HLA class I antigen processing and presentation pathway. Furthermore, known mechanisms of the adjuvant activity of $Al(OH)_3$ were elucidated in more detail such as inflammasome and complement activation, homeostasis and HLA-class II upregulation, possibly related to increased IFNγ gene expression. Altogether, our study revealed which immunological pathways are activated upon stimulation of monocytes with $Al(OH)_3$, refining our knowledge on the adjuvant effect of $Al(OH)_3$ in primary monocytes.

Significance: Aluminum salts are the most used adjuvants in human vaccines but a comprehensive understanding of the working mechanism of alum adjuvants *at the molecular level* is still elusive. Our Systems Vaccinology approach, combining complementary molecular biological, immunological and mass spectrometry-based techniques gave a detailed insight in the molecular mechanisms and pathways induced by $Al(OH)_3$ in primary monocytes. Several novel immunological relevant cellular pathways were identified: type I interferon secretion potentially induced by TLR and/or NOD like signaling, the activation of the inflammasome and the HLA Class-I and Class-II antigen presenting pathways induced by IFNγ. This study highlights the mechanisms of the most commonly used adjuvant in human vaccines by combing proteomics, transcriptomics and cytokine analysis revealing new potential mechanisms of action for $Al(OH)_3$.

1. Introduction

Since 1926, colloidal aluminum salts are known for their adjuvant features, when Glenny et al. discovered that diphtheria toxoid adsorbed to aluminum salts showed a significantly higher antibody titer against the toxoid compared to antigen alone [1]. Since then, aluminum salts

☆ Data availability: the authors confirm that all data is available without any restrictions. Proteome Data is available via ProteomeXchange with identifier PXD008452.

* Corresponding author.
E-mail address: hugo.meiring@intravacc.nl (H.D. Meiring).
[1] Current address: Istituto Clinico Humanitas IRCCS, Milan, Italy.
[2] Current address: Centre hospitalier Universitaire, Vaudois, Switzerland.
[3] Current address: Immunocore, Ltd. Abingdon, United Kingdom.

https://doi.org/10.1016/j.jprot.2017.12.021
Received 13 July 2017; Received in revised form 21 December 2017; Accepted 29 December 2017
Available online 06 January 2018

have been widely used as vaccine adjuvants, even though the mechanism of action has remained largely unknown. Shortly after Glenny et al. discovered its potential, it was observed that the clearance of aluminum salt-adsorbed toxoids was delayed compared to non-adsorbed toxoids [2]. This observation was the basis for the theory that antigen-aluminum salt aggregates form a depot at the site of injection, leading to a slow release of the bound antigen. However, when the aluminum salt deposit was removed at various time points, the immune response was not compromised, suggesting that this is not the only mechanism by which aluminum salts increase the immune response to antigens [3]. It was shown that antigens desorb rapidly from $AlPO_4$ as well as $Al(OH)_3$ after administration, explaining that even when the aluminum salt-deposit is removed, an antibody response is still created [4]. It was demonstrated by flow cytometric analysis that $Al(OH)_3$ causes the differentiation of monocytes to antigen-presenting dendritic cells, which then can elicit a specific immune response in the presence of an antigen [5–7]. $Al(OH)_3$ has been shown to steer the $CD4^+$ T cell response towards a T helper type 2 (Th2) response and induces the recruitment of immune cells (*e.g.* dendritic cells, inflammatory monocytes, eosinophils, neutrophils natural killer cells and $CD11^+$ cells) to the site of injection [7–12].

Additional mechanisms for the adjuvant effect of $Al(OH)_3$ have been described: for example, the activation of the NLRP3 inflammasome, as identified by both *in vivo* and *in vitro* studies [12–15]. Inflammasome activation results in the secretion of IL-1β, a pro-inflammatory cytokine and potent inducer of the adaptive immune response and Th2 polarization [13, 15, 16]. The inflammasome, *in vitro*, appeared to be critical for $Al(OH)_3$ dependent IL-1β secretion and antibody responses. *In vivo* however, there is conflicting data about the necessity of the inflammasome to induce a humoral response [13, 15, 17]. Complement activation is another mechanism involved in the adjuvant activity of $Al(OH)_3$ [12, 18]. The release of Danger Associated Molecular Patterns (DAMPs) like uric acid and host DNA, is induced by $Al(OH)_3$ [13, 19, 20]. Uric acid is involved in T cell priming and humoral responses [13, 15]. Besides this, uric acid can also activate the inflammasome *in vitro* [15, 21]. However, *in vivo* IL-1β production did not depend on the presence of uric acid [14, 15]. Uric acid is involved in the influx of inflammatory monocytes to the site of injection as is MyD88, since MyD88-deficient mice showed a significant reduction of the influx of inflammatory monocytes [13]. Even though MyD88 appears to be dispensable for antibody production there is a role in the adjuvant activity of $Al(OH)_3$ [13]. DNA is also involved in the adjuvant activity of $Al(OH)_3$ [19]. DNA can result in the secretion of IL-1β or in the secretion of IFNβ and enhances MHC class II antigen presentation [19, 20]. In conclusion, there are many potential mechanism described for the adjuvant activity of $Al(OH)_3$. A comprehensive study compiling transcriptome data with proteome data would make it possible to follow pathways in more detail and create an overview of which pathways are actually activated by the $Al(OH)_3$ adjuvant.

In this study, we investigated the $Al(OH)_3$-induced innate cell response at the transcriptome and proteome level, aiming to further complete the overview of molecular pathways and cellular processes involved in the adjuvant effect of $Al(OH)_3$. Primary monocytes were chosen as a model, since these prominent mononuclear phagocytes play an important role in tissues when activated, bridging the innate and adaptive immune responses [22, 23]. Besides there known differentiation into monocyte derived dendritic cells (MDDCs), monocytes can also enforce their antigen presenting role to T cells in response to various stimuli as recently reviewed [24]. In the current study the effect of $Al(OH)_3$ on monocytes will be investigated. The combination of transcriptome/proteome analyses and cytokine measurements enabled the comprehensive identification of molecular pathways in $Al(OH)_3$-stimulated monocytes, further clarifying the mechanism by which $Al(OH)_3$ works.

2. Materials and methods

2.1. Ethics statement

This study was conducted using blood donations, provided by the National Institute for Public Health and the Environment (Bilthoven, The Netherlands), for primary cell isolation. The blood donations for this research goal were specifically approved by the accredited Medical Research Ethics Committee (MREC), METC, Noord-Holland in The Netherlands. The study was conducted according to the principles expressed in the Declaration of Helsinki and written informed consent was obtained from all blood donors before collection and use of their samples. Blood samples were processed anonymously. All human primary cells described in this study were obtained by the rules of this ethical statement.

2.2. Reagents used in cell stimulation

Aluminum hydroxide (Alhydrogel 2%; Brenntag; Frederikssund; Denmark) is referred to as $Al(OH)_3$. Lipopolysaccharide (LPS) from *E. coli* K12 (Invivogen; San Diego; California; USA) was used as positive control and is referred to as LPS.

2.3. Isolation and stimulation of monocytes

Peripheral blood derived from 7 healthy adult donors and obtained as described in the ethical statement, was used for monocyte isolation. First, peripheral blood mononuclear cells (PBMCs) were obtained by gradient centrifugation at 1,000 × *g* for 30 min on Lymphoprep (Nycomed; Zurich; Switzerland). Second, monocytes were isolated from the PBMC fraction using MACS in combination with anti-CD14 MACS beads (Miltenyi Biotech; Bergisch Gladbach; Germany). Purity check by flow cytometric analysis of CD14 cell surface expression was performed and only if the purity of the monocyte population was ≥95% the cells were used for proteome and transcriptome analysis.

Monocytes were cultured in a 24-well culture plate (0.6×10^6 cells/ml, 1 ml/well) in RPMI (Gibco/Thermo Fisher; Waltham; Massachusetts; USA) containing 10% Fetal Calf Serum (FCS) (Hyclone), 100 units/ml of penicillin (Gibco) 100 units/ml streptomycin (Gibco), and 2.92 mg/ml L-glutamin (Gibco), hereafter referred to as monocyte culture medium. Isolated monocytes were either left unstimulated in monocyte culture medium, or were stimulated with 500 μl of LPS or $Al(OH)_3$ in monocyte culture medium with a final concentration of 0.1 μg/ml or 10 μg/ml, for 24 or 48 h respectively, based on the study of Ulanova et al. [5].

After incubation, culture supernatants were collected and stored at −80 °C for cytokine analysis. Small aliquots were taken from cell suspensions from each donor per time point for flow cytometry analysis.

For proteome analysis, the cells of at least one well per condition per time point per donor (three individuals) were washed with PBS, before adding 500 μl lysis buffer (4 M Guanidine·HCl in phosphate buffer pH 7.5) (Sigma Aldrich; St Louis; Missouri; United States).

For transcriptome analysis, the cells of at least one well per condition per time point per donor (5 individuals) were placed in 350 μl of RLT buffer (Qiagen; Venlo; The Netherlands). The samples for proteome and transcriptome analysis were stored at −80 °C.

2.4. Generation and stimulation of primary Monocyte-Derived Dendritic Cells (MDDCs)

Monocytes from the peripheral blood of 6 donors, obtained as described in the ethics statement, were cultured in a 24-well culture plate (0.4×10^6 cells/ml, 1 ml/well) in DC culture medium, *i.e.* IMDM (Gibco) containing 1% FCS, 100 units/ml penicillin, 100 units/ml streptomycin, 2.92 mg/ml L-glutamine (Gibco), 500 units/ml GM-CSF (Prepotech; Rocky Hill; New Jersey; USA) and 800 units/ml IL-4

(Sanquin; Amsterdam; The Netherlands) for 6 days. On day 6, the immature MDDCs (iMDDCs) were either left unstimulated, or were stimulated for 48 h with 250 µl of LPS or $Al(OH)_3$ in DC culture medium containing 250 units/ml GM-CSF, with a final concentration of the stimulus of 0.1 µg/ml or 10 µg/ml. After 48 h, supernatant were stored at −80° for cytokine analysis. The stimulated MDDCs were harvested and suspended in FACS buffer. Aliquots were taken from cell suspensions for flow cytometric analysis which was used as a quality control for the cell culture procedure. Flow cytometric analysis of monocytes was used as a quality control for the cell culture procedure. LPS served as a positive control and performed as expected, by inducing CD80 expression (Supplementary S1). Samples were only used for further analysis if the monocytes were at least 95% pure.

2.5. Culture and stimulation of THP-1 cells

The human monocytic cell line THP-1 (ATCC; Teddington; Middlesex; U.K.) was used for verification experiments of leads identified in primary monocytes. THP-1 cells were cultured according to the supplier's protocol with the addition of 100 units/ml penicillin, 100 µg/ml streptomycin and 300 µg/ml L-glutamine to the medium, hereafter referred to as THP-1 culture medium, in culture flasks.

Cells were primed with 300 ng/ml phorbol 12-myristate 13-acetate (PMA) (Sigma Aldrich) for 24 h, after which the medium was discarded and new medium without PMA was added. After 24 h in the refreshed medium, the following stimulations were performed: mock, 50 or 100 µg/ml $Al(OH)_3$ (based on literature [5, 14] and preliminary experiments). Each of these conditions was performed in the presence and absence of 25 µg/ml glybenclamide (Invivogen). An additional cell batch was left completely unstimulated and unprimed. Twenty-four and 48 h after stimulation, supernatants of cultures were harvested and used for an IL-1β ELISA.

2.6. Flow cytometric analysis

For purity analysis, isolated monocytes were stained with PE-conjugated anti CD14 clone (H5E2). Cultured monocyte and MDDC cell suspensions were stained with PE-conjugated anti-CD40 (BD Biosciences; clone 5C3), APC-conjugated anti-CD80 (BioLegend; clone 2D10), FITC-conjugated anti-CD83 (BD Biosciences; clone HB15e), Pacific Blue-conjugated anti-CD86 (BioLegend; clone IT2.2), HLA-DR FITC (Sanquin; clone L243) and finally with LIVE/DEAD Fixable Aqua Dead Cell Stain Kit (Invitrogen) for 30 min at 4 °C. The cells were washed in FACS buffer and fixed in FACS buffer containing 1% paraformaldehyde (PFA). Data were acquired on a FACS Canto II (BD Biosciences) and analyzed using FlowJo software (Tree Star) by comparing the MFI of the stained control with the MFI of the stained stimulus. The data were corrected for the percentage autofluorescence determined in verification experiments by comparing the unstained stimulated with the stained stimulated cells for each stimulus.

2.7. mRNA expression analysis

mRNA was isolated from monocyte samples using the RNeasy mini kit (Qiagen) according to the animal cell spin protocol provided. Isolated RNA concentrations and purities were determined by the spectrophotometric analysis of the 260-nm and 280-nm absorbance on the Nanodrop 2000 (Thermo Fischer). Subsequently, cDNA synthesis was performed with the RT cDNA synthesis kit (Qiagen) and the RT preAMP pathway primer mix, innate and adaptive immunity comprising primers for 89 functional RNA species and controls, on 12 ng of RNA per condition (Qiagen). cDNA was subsequently frozen at −20 °C.

qPCR was performed by using the Innate and Adaptive Immune Responses RT^2 Profiler PCR Arrays (PAHS 052ZC) (Qiagen) (Supplementary S2) on a qPCR apparatus (ABI step one plus; Applied Biosystems; Foster City; California; USA) with a melt curve determination as a quality control, included in the measurement.

qPCR data were analyzed with the qPCR statistical web software from Qiagen. Gene expression was normalized to HPRT1 as housekeeping gene, after which the fold change was calculated according to the manufacturer's protocol. Fold change-values greater than one indicate an upregulation, in which the fold regulation is equal to the fold change. Fold change-values less than one indicate a downregulation in which the fold regulation is the negative inverse of the fold change. For donor F (with three technical replicates), *p*-values were calculated based on a Student's *t*-test of the replicate values for each gene in the control group and treatment group. Genes were considered regulated if p-value < 0.05 and a two-fold change in expression occurred. We validated technical replicate reproducibility with the first donor. The Coefficient of Variation (CV) between technical replicates was 3.5% for all transcriptome data and all the genes that met the two fold difference criterion also had a p-value < 0.05. Therefore, for the other four donors we used one technical replicate and considered genes regulated if they met the two-fold difference criterion. Overall, genes were considered regulated by $Al(OH)_3$ if they showed a two-fold up- or down-regulation in at least three out of five donors, or were regulated in two donors with a clear trend in at least one other.

LPS served as a control for the time point and for potential artifacts [25] of the cell isolation with CD14 beads, by determining if LPS-related genes were indeed increased. It was confirmed that LPS-related genes were indeed increased after 24 h (Supplementary S3), indicating that the time point can indeed be used and that artifacts (no induction of LPS-related genes) might not play a role here.

2.8. Protein isolation

Monocytes were lysed by adding 500 µl 4 M Guanidine·HCl in 100 mM phosphate buffer (pH = 7.5) to the culture plate and incubated for 2 h at 4 °C. During these 2 h, the cells were subjected to a freeze-thaw step. The protein concentrations were determined with a BCA protein assay (Pierce biotechnology; Waltham Massachusetts; USA) according to the manufacturer's protocol. Lysed cells were stored at −80 °C in a culture plate.

2.9. Protein digestion

Protein samples from monocytes were diluted 4 times with 100 mM phosphate buffer pH 7.5 to reduce the Guanidine·HCl content to 1 M and adjust the pH to 7.5. Proteins were digested at 37 °C with Lys-C (Roche; Basel; Switzerland) in an enzyme-to-substrate ratio of 1:10 (*w/w*). After 4 h, fresh Lys-C was added in a 1:10 (w/w) ratio for an overnight incubation.

2.10. Protein labeling in monocyte samples

Following the protein digestion, aliquots from the six monocytes samples per donor (three donors) were taken containing equal protein amounts and per condition labeled using tandem mass tag labeling 6-plex (TMT(6), Thermo Fisher). For donor A 25 µg per condition per time point was labeled, for donor B 50 µg protein per condition per time point was labeled and for donor C 25 µg protein and 10 µg per condition was labeled at 24 and 48 h, respectively. Labeling was performed on Solid Phase Extraction (SPE) columns (Waters; Milford; MA; USA). The SPE columns were equilibrated as described by the manufacturer and washed with 100 mM phosphate buffer pH 7.5. The digested protein samples were loaded onto 6 separate SPE columns using a vacuum manifold (Waters) and washed with 100 mM phosphate buffer pH 7.5. The TMT-label (0.8 mg per TMT-label) was reconstituted in 41 µl acetonitrile (AcN) according to the supplier's protocol. The AcN concentration was reduced to a maximum of 2.5% (*v/v*) with 100 mM phosphate buffer pH 7.5. The individual TMT labels were loaded onto the 6 SPE columns, leaving 0.5 ml reagent on top of the column for a

30 min incubation, fresh label was added for another 30 min of incubation, after which the columns were washed with water containing 0.5% formic acid (FA). The six samples were eluted with 90% AcN containing 0.5% FA, pooled, dried by centrifugal evaporation and reconstituted in water containing 0.1% trifluoroacetic acid (TFA).

2.11. SCX fractionation

Pooled and labeled monocyte-derived protein samples were purified by Strong Cation exchange (SCX) as described previously [26]. The system comprised a HyperCarb trapping column (200 μm I.D. × 5 mm length, 7 μm particle size) and an SCX column (200 μm I.D. × 11 cm length PolySULFOETHYL Aspartamide, 5 μm, PolyLC), both made in-house. The gradient was 12 min at 100% solvent A (water + 0.5% HOAc), after which a linear gradient started to 100% solvent B (250 mM KCl + 35% AcN + 0.5% HOAc in water) in 16.5 min, followed by a second linear gradient to 100% solvent C (500 mM KCl + 35% AcN + 0.5% HOAc in water) in 16.5 min at a column flow rate of 2 μl/min. Twenty-six 4-μL fractions were collected. Fractions were analyzed for peptide content during fractionation using UV. The peptide-containing fractions were subjected to nanoscale LC-MS analysis.

2.12. LC-MS/MS analysis

Peptide separation was performed on a Proxeon Easy-nLC 1000 system (Thermo Scientific). Peptides were trapped on a double-fritted trapping column Reprosil C18 (Dr. Maisch; Ammerbuch; Germany; df = 3 μm, 2 cm length × 100 μm I.D.) and separated at a column temperature of 40 °C on an analytical column Poroshell 120 EC-C18 (Agilent; df = 2.7 μm, 50 cm length × 50 μm I.D.) both packed in house. Both columns contained a 1-mm length KASIL frit prepared as described by Meiring et al. [27], to retain the packing bed. The second KASIL frit, upstream in the trapping column, was made the same way after flushing the packing bed with helium. Solvent A was 0.1% FA in MilliQ water and solvent B was 0.1% FA in AcN (Biosolve). The peptides were separated in 143 min (10 min at 2% B for peptide loading onto the trapping column, followed by a 118-minute gradient from 2% to 30% B and 5 min at 70% B) in a non-linear optimized gradient [28]. After 128 min, the system was kept at 5% B for 15 min to equilibrate the column. The column effluent was electro-sprayed directly into the MS using a gold-coated fused silica tip with a 5-μm TipID and a spray voltage of 1.8 kV.

Mass spectrometric data were acquired on a Tribrid-Orbitrap Fusion (Thermo Fisher Scientific), where the full scan (MS^1) spectra were acquired with a scan range of *m/z* 350–1500 Da at 120 K resolution (FWHM) with an Orbitrap readout. The Automatic Gain Control (AGC) for the MS^1 was set to 200,000 and the maximum injection time to 50 ms in top speed mode with a duration of 3 s, where precursor ions with an intensity of > 5000 were selected for fragmentation (MS^2). Charge states between 1 and 7 were selected. MS^2 was performed using Collision-Induced Dissociation (CID) in the linear ion trap with a normalized collision energy of 35%. The AGC for the MS^2 was set to 10,000 and the maximum injection time to 35 ms. Synchronous-Precursor-Selection was enabled to include up to 10 MS^2 fragment ions. These ions were further fragmented by Higher energy Collision Dissociation (HCD) with a normalized collision energy of 50%. TMT reporter ions were analyzed in the Orbitrap analyzer, with the AGC set to 100,000 and a maximum injection time of 120 ms.

Proteomics data were analyzed with Proteome Discoverer 2.1 (PD 2.1) (Thermo Fisher Scientific) using default settings unless stated otherwise. Precursor mass tolerance was set to 5 ppm, MS/MS scans were searched against the human Uniprot database (Nov 2014), containing 23,048 entries, using the Sequest HT search engine with full enzyme specificity for Lys-C, with *b* and *y* type ions enabled for CID and HCD data with a fragment mass tolerance of 0.5 Da. The data was searched with Aspargine deamidation and Methionine oxidation as dynamic modifications. TMT(6) was set as a static modification on the Lysine residues and the peptide N-termini. For relative quantitation, the quantification node was used with TMT(6) as defined quantification method and an integration tolerance of 0.2 Da. A decoy database defined in the Percolator node was used to validate and filter the peptide-to-spectrum matches with a False Discovery Rate (FDR) of < 5%. Only medium (FDR < 5%) and High (FDR < 1%) confident identified proteins were used in the further data analysis.

The protein data from the SCX fractions of an individual donor were combined by PD 2.1 in a consensus report, resulting in one output table per donor/technical replicate. If multiple entries occurred for the same protein, based on Uniprot and NCBI data, the ratios given by Proteome Discoverer were Log2-transformed and averaged for further analysis. Next, a median correction normalization was performed. For donor C, three technical replicates of the medium control and $Al(OH)_3$-stimulated culture conditions were measured (their median CV was 10.5% for the full proteomics data set) and these were combined into a single average value for this donor to make sure each donor is weighed equally in further analysis. For donors A and B, one sample per condition was analyzed. Data of three biological replicates (donors) were compared and proteins that were upregulated or downregulated by 1.5 fold or more in at least two out of three biological replicates were considered substantially regulated. These regulated proteins were imported in STRING (string.embl.de) [29], to identify enriched pathways in these regulated protein sets (FDR < 0.05), within Gene Ontology (GO) biological processes.

The mass spectrometry proteomics data have been deposited to the ProteomeXchange Consortium *via* the PRIDE [30] partner repository with the dataset identifier PXD008452.

2.13. IL-1β ELISA

IL-1β levels in culture supernatants were determined using the Human IL-1 beta/IL-1F2 DuoSet ELISA (R&D systems; McKinley; Minneapolis; USA.). The analysis was performed according to the manufacturer's protocol and recorded on a Synergy MX (Biotek; Winooski Vermont; USA).

ELISA data were analyzed with GraphPad Prism®. Significance of difference was determined using a 2-way ANOVA and a Tukey's multiple comparison test with an Alpha of 0.05.

3. Results

3.1. $Al(OH)_3$ induces changes in cell surface markers on monocytes but not on Immature monocyte derived dendritic cells

When immature monocyte-derived dendritic cells (iMDDCs) were stimulated with $Al(OH)_3$, no significant changes in cell surface marker expression were observed, as determined by flow cytometry, whereas LPS stimulation resulted in the upregulation of CD40, CD80 and CD83 (Supplementary S4). Based on the limited effect of $Al(OH)_3$ on iMDDCs, further detailed analyses were only performed using monocytes.

The effect of incubation of monocytes with $Al(OH)_3$ on their cell surface marker expression was investigated at the level of gene expression (with targeted transcriptomics) and protein identification and quantification. $Al(OH)_3$ stimulation upregulated gene expression of, *CD80*, and *CD8A* in monocytes compared to control cells after 24 h of stimulation. Gene expression of *CD14*, a typical monocyte marker that is lost upon differentiation into iMDDCs and linked to LPS stimulations [31], was downregulated in $Al(OH)_3$-stimulated monocytes after 24 h (Fig. 1), while gene expression was upregulated in LPS-stimulated monocytes (Supplementary S3, S5). Moreover, at the protein level (analyzed with quantitative mass spectrometry) CD14 was downregulated after 48 h of $Al(OH)_3$ stimulation (Supplementary S6, S7). $Al(OH)_3$ stimulation of monocytes resulted in an increased protein

expression of activation markers CD9 and CD71 (TRFC) after 48 h (Table 2 and Supplementary S6, S7) (please note: these markers were not analyzed using targeted transcriptomics). These transcriptome and proteome results confirmed that in an $Al(OH)_3$-stimulated monocyte population cells became activated and start changing their cell surface marker phenotype including the loss of CD14 expression.

3.2. *Al(OH)$_3$ induces changes in immunogenic genes upon monocyte stimulation*

Targeted transcriptome analysis of monocytes was performed on an array of 96 genes, comprising innate and adaptive immune system genes, housekeeping genes and control genes (Supplementary S2). In total, 89 functional gene-transcripts could be measured, of which 40 genes were found to be upregulated and 5 genes were downregulated (Table 1 and Fig. 1). Some donor variation was observed since genes were not always differentially regulated in all donors. Fig. 1 is most representative for all donors used.

3.3. *Quantitative proteomics reveals up and downregulation of homeostatic and immunogenic processes after Al(OH)$_3$ stimulation of monocytes*

Quantitative proteome analysis of $Al(OH)_3$-stimulated monocytes resulted in the identification of over 4000 unique proteins, of which 3000 proteins could be relatively quantified. About 200 proteins were upregulated and about 190 proteins were downregulated in $Al(OH)_3$-stimulated monocytes compared to unstimulated monocytes (Supplementary S6–S10). Some of these proteins could be matched to the transcriptome data, *e.g.* HLA-A, HLA-E and CD14 (Table 2). Cytokines were not identified in the lysates. However, several cytokine inducible proteins were detected in the lysates (*e.g.* Mx1, Mx2 and IFIT3). These proteins are induced by IFNβ [32–34].

Over-representation analysis of GO terms, revealed the involvement of various biological processes (Figs. 2 and 3). A comprehensive overview of all differentially regulated proteins and enriched GO terms is represented in Supplementary S7 and S8–10. Immune processes, like *antigen processing and presentation* and *innate immune response* were over-represented as well as processes involved in homeostasis like *metabolic processes*, *localization* and *transport*(Fig. 2). Specific pathways that were induced after 24 h were related to *localization* and *copper homeostasis*: specified proteins related to this process were *e.g.* copper-transporting ATPase 2 (ATP7B) and Amyloid-beta A4 (APP). After 48 h of stimulation, additional GO terms were enriched in the upregulated protein sets as compared to 24 h of stimulation including: *intracellular transport processes* (*e.g. protein transport*, *protein localization*) and *response to stress* (Fig. 3B). Processes related to cell death were also increased after $Al(OH)_3$ stimulation (*programmed cell death*). A complete overview can be found in Supplementary S8–S9.

Within the set of downregulated proteins after 24 h of $Al(OH)_3$ stimulation, no GO terms were over-represented. However, in the data set representing downregulated proteins after 48 h, over-representation of various GO terms was identified *i.e. blood coagulation*, *inflammatory response*, *regulation of immune system process* and *response to stress* (Supplementary S10). These data show that $Al(OH)_3$ regulated both processes involved in homeostasis as well as in the immune response.

3.4. *IL-1β production as a consequence of Al(OH)$_3$ stimulation is partially inflammasome dependent*

Inflammasome-related gene expression was increased in transcriptome analysis after 24 h of $Al(OH)_3$ stimulation, *i.e. NOD1 and IL-1R1*, while *CASP1* and *MyD88* were upregulated in two donors (Fig. 1). IL-1β ELISA analysis in the culture supernatant of two donors showed a trend towards increased IL-1β secretion (Supplementary S11). Cytokine analysis with an IL-β ELISA in THP-1 cells confirmed the upregulation of IL-1β after 48 h (Fig. 4 and Supplementary S12).

To investigate the involvement of the inflammasome in IL-1β production upon $Al(OH)_3$ stimulation in more detail, THP-1 cells (a human monocytic cell line) were differentiated into macrophages by addition of PMA and stimulated with 50 μg/ml of $Al(OH)_3$ in the presence and absence of the inflammasome blocker glybenclamide. Measurement of IL-1β in cell culture supernatants of THP-1 cells revealed that IL-1β secretion upon $Al(OH)_3$ stimulation decreased in the presence of glybenclamide (Fig. 4 and Supplementary S12). A similar trend was observed when tested in primary monocytes: one donor with blocking (donor A) and one donor without blocking experiment (donor B) (Supplementary S11). However, this response was less pronounced if compared to the response in PMA-primed THP-1 cells. The loss of IL-1β production upon glybenclamide addition provided evidence that the IL-1β production of $Al(OH)_3$-stimulated monocytic cells is indeed partially dependent on the activation of the inflammasome.

3.5. *Al(OH)$_3$ activates the complement system*

Our proteomics data of $Al(OH)_3$-stimulated primary monocytes identified the altered expression of proteins from all complement pathways: C4 (lectin pathway), C8 (alternative pathway), and C5aR (classical pathway) were significantly upregulated after 24 h of stimulation (Table 2 and Supplementary S7). In addition, gene expression of *C3* was upregulated and *CASP1* was upregulated in two donors (Table 1).

3.6. *Al(OH)$_3$ promotes the production of Th2 and Th1 related cytokines*

Notably, in $Al(OH)_3$-stimulated monocytes, the Th1-associated gene *IFN*γ [35, 36] was upregulated after 24 h (Fig. 1 and Supplementary S5). Proteins involved in the response to IFNγ, IFNγR1 and IFI30, were also upregulated (Supplementary S7). Other cytokine genes increased after $Al(OH)_3$ stimulation, were *IL-2*, *IL-5*, *IL-17A*, *IL-23A and IFNβ* (Fig. 1, Table 1 and Supplementary S5). Interferon-induced protein with tetratricopeptide repeats 3 (IFIT3) and the interferon-induced GTP-binding proteins Mx1 and Mx2 were also upregulated (Table 2). In addition, increased expression of the Th2 polarizing gene *IL-4* was observed, after 24 h of stimulation (Table 1 and Fig. 1). However, in the presence of the Th1-associated gene *IFN*γ, which was also increased after 24 h of stimulation.

3.7. *Stimulation with Al(OH)$_3$ increases the chemotactic capacity of the monocytes*

Transcriptome data showed that $Al(OH)_3$-stimulated monocytes regulated mechanisms to attract other immune cells. The gene expression of *CCL2* was upregulated in $Al(OH)_3$-stimulated monocytes (Table 1); this gene encodes for a molecule involved in monocyte trafficking. $Al(OH)_3$ stimulation also induced the expression of chemokine receptors *CCR6* and *CCR8* (Table 1).

3.8. *Al(OH)$_3$ induces upregulation of components of the HLA processing and presentation pathways in monocytes*

The upregulation of HLA class II pathways in monocytes induced by $Al(OH)_3$ was observed at the level of the proteome. The pathway antigen processing and presentation by HLA class II was enriched in the upregulated protein data set of $Al(OH)_3$-stimulated monocytes. HLA class II-related upregulated proteins included Legumain [37–39] and Cathepsin D, S and L (Table 2 and Supplementary S7) [40]. mRNA expression of *IFN*γ was upregulated as was the protein expression of IL-3R, both synergizing in increasing HLA class II expression [41, 42].

In addition to HLA class II pathway upregulation, induction of HLA class I-related genes and proteins was observed. $Al(OH)_3$ stimulation of monocytes increased gene and protein expression of HLA-A and HLA-E, as well as the gene expression of *β2M* compared to controls (Table 1 and

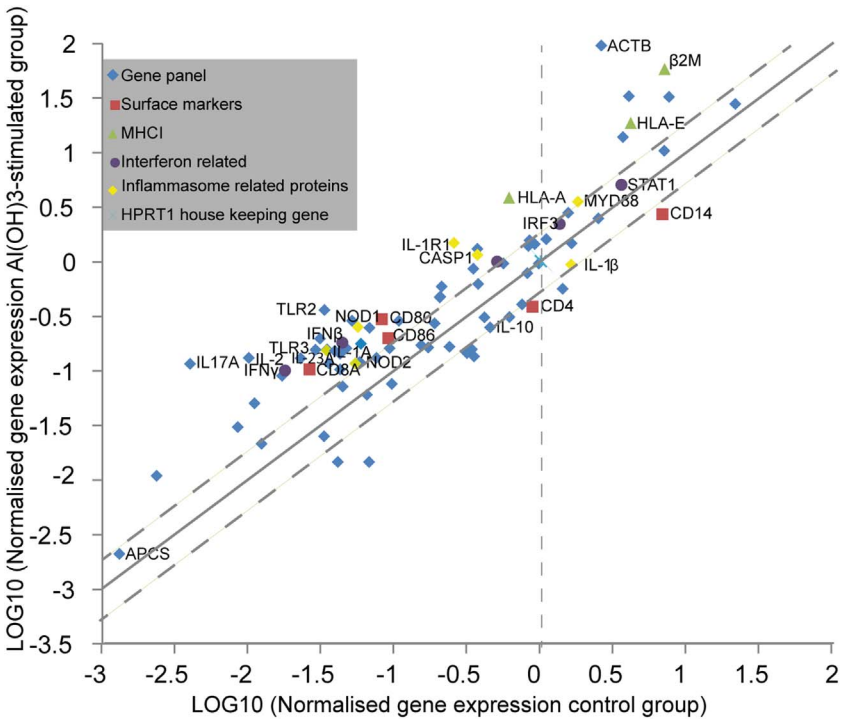

Fig. 1. Gene expression profile of $Al(OH)_3$-stimulated monocytes after 24 h.
Gene expression was normalized to a housekeeping gene. This figure depicts the LOG10(normalized) gene expression profile after 24 h of $Al(OH)_3$ stimulation (10 μg/ml) compared to the control, of two representative biological replicas (for an overview of all the altered genes in three out of five donors see Table 1). The genes above the upper dotted line are significantly upregulated by at least a factor of 2 as a result of the $Al(OH)_3$ stimulation, while the genes below the lower dotted lines are downregulated by at least a factor of 2 due to the $Al(OH)_3$ stimulation.

Fig. 1). HLA class I-related proteins were also upregulated upon $Al(OH)_3$ stimulation *i.e.* heat shock protein 90 (HSP90) and Minor Histocompatibility Complex HM13 (Table 2).

3.9. $Al(OH)_3$ stimulation of monocytes induces IFNβ secretion potentially by upregulating TLR or NOD like signaling

$Al(OH)_3$ stimulation of monocytes resulted in a significantly increased *IFNβ* gene expression ($p < 0.01$). Protein expression of proteins downstream of IFNβ: *i.e.* Mx1, Mx2, and IFIT3 was increased in $Al(OH)_3$-stimulated monocytes (Supplementary S7), as was the gene expression of *Mx1*. This provides evidence that IFNβ indeed has been secreted, since these proteins would otherwise not have been increased. These proteins could be induced by IFNβ *via* STAT1. Indeed, gene expression of *STAT1* was upregulated in $Al(OH)_3$-stimulated monocytes (Fig. 1 and Supplementary S5). These data confirm the secretion and consumption of IFNβ.

Indications of IFNβ transcription were also found since the gene expression of *IRF7* a key transcriptional regulator was found to be increased (Fig. 1). *IRF3* gene expression was increased in two donors. Genes involved in the pathways *via* which IRF7 can mediate the induction of type I interferons were increased, *i.e. TICAM1* and *IRAK1* while *MyD88*, and *TRAF6* clearly trended towards upregulation (Table 1 and Supplementary S5) [43]. The protein TBK1 in the IRF7 signaling pathway was identified at the level of the proteome but was not increased (Supplementary S6). Upstream of both *MyD88/IRAK1* and *TICAM/TRAF6*, TLR and NOD signaling could be involved, although $Al(OH)_3$ is not a ligand for both TLRs and NOD1. However, $Al(OH)_3$ induced cell stress and cell death (Supplementary S8 and S9) [13, 16, 19], resulting in the release of DAMPs/endogenous ligands. These

Table 1
Genes differentially expressed upon $Al(OH)_3$ (10 μg/ml) stimulation of monocytes.

Pattern recognition receptors (PPRs) and signaling	Cytokines and chemokines	Cytokine and chemokine receptors	Surface markers	Transcription factors	Complement system	Antigen presentation	Others
NOD1[2]	CCL2[2]	CCR6[2]	CD8A[2]	FoxP3[2]	C3[2]	β2M[2]	ACTβ[2]
TLR2[2]	CSF2[2]	CCR8[2]	CD80[2]	GATA3[2]	*CASP1*[2]	HLA-A[2]	CD40LG[2]
TLR3[2]	IL-2[2]	CXCR3[2]	*CD4*[1]	*IRF3*[2]		*HLA-E*[2]	CRP[2]
MYD88[2]	IL-4[2]	IL-1R1[2]	CD14[1]	IRF7[2]			MPO[2]
IRAK1[2]	IL-5			*TBX21*[1]			MX1[2]
TICAM1[2]	IL-17A[2]						RAG1[2]
DDX58[2]	IL-23A						STAT1[2]
	IFNαR1[2]						STAT3[2]
	IFNβ1[2]						*S*TAT6[2]
	IFNγ[2]						TYK2[2]
	TNF[2]						*TRAF6*[2]
	IL-1β[1]						MAPK1[2]
	IL-18[1]						MAPK8[2]
							RORC[2]
							LY96[2]
							LYZ[1]
							NLRP3[1]

Italic genes: genes that are upregulated/downregulated in 2 donors and a trend towards upregulation in at least one additional donor.
[1] Annotated genes that are downregulated by at least a factor of 2 in at least 3 donors.
[2] Annotated genes that are upregulated by at least factor of 2 in at least 3 donors.

Table 2
Selection of proteins and their fold changes after 24 and 48 h of $Al(OH)_3$ (10 μg/ml) stimulation compared to control in primary monocytes.

Accession number	Protein	Fold changes after 24 h	Fold changes after 48 h
P05534	HLA-A	1.05	15.53
P13747	HLA-E	2.65	15.01
Q8TCT9	HM13	2.11	4.01
Q99538	LGMN	2.20	3.08
P07339	CTSD	2.43	3.35
P07711	CTSL	7.04	6.85
P25774	CTSS	1.22	1.71
O60911	CSTV	2.53	2.39
P21926	CD9	1.57	2.82
P08571	CD14	0.67	0.20
P02786	TFRC	1.47	3.32
P20591	MX1	1.36	1.62
P20592	MX2	1.26	1.72
P13284	IFI30	2.31	1.49
O14879	IFIT3	1.62	2.53
P26951	IL3RA	3.37	90.58
P15260	IFNgR1	2.02	3.37
Q9UHD2	TBK1	0.92	0.99
P0C0L4	C4	1.86	1.74
P21730	C5aR1	1.50	1.97
P07357	C8a	2.64	1.77
P07358	C8b	6.86	0.93

endogenous ligands can bind various receptors leading to the secretion of type I interferons. Gene expression of a subset of these DAMP sensors was identified in this data set, specifically DDX58, (no further pathway evidence identified) TLR2 (upregulated in two donors but downregulated in one), TLR3 (upregulated in four donors) and NOD1 (in two donors tending towards upregulation in at least one more) (Fig. 1). TLR3 can be activated by endogenous mRNA [44–46] resulting in the secretion of type I interferons, *via* the induction of TICAM1, TRAF6, TBK1 and IRF7 [44, 45, 47]. TLR2 (upregulated in two donors and downregulated in one donor) can be induced by endogenous ligands and induce the secretion of type I interferons *via* the pathway described by Dietrich et al. [48]. NOD1 can also be induced by endogenous ligands and results in the formation of type I interferons [49, 50]. These data indicate the TLR signaling and NOD1 signaling could be involved in the induction of type I interferons by DAMP sensing.

Although involvement of other DNA sensors cannot be excluded, hypothetical $Al(OH)_3$-induced pathways resulting in the release of type I interferons, based on the data described and the literature are depicted in Fig. 5.

4. Discussion

A comprehensive analysis of the effects of $Al(OH)_3$ on monocytes revealed two novel cellular processes to be involved in the adjuvant action of $Al(OH)_3$: first, IFNβ secretion *via* NOD1 or TLR signaling and second, the upregulation of antigen processing and presentation *via* HLA class I-related proteins, potentially leading to more antigen processing and presentation when an antigen is present. Together with a deeper elucidation of known $Al(OH)_3$-affected mechanisms, these novel processes emphasize that $Al(OH)_3$-stimulated monocytes prepare for a pro-inflammatory function and antigen presentation in the immune response [22–24].

Known mechanisms of $Al(OH)_3$ (as reviewed by He et al. [12]) were elucidated in more detail: inflammasome activation, complement activation, cytokine induction, monocyte activation and differentiation and induced HLA-class II activation possibly due to increased *IFN*γ gene expression. It is noteworthy that *IFN*γ gene expression is induced as a result of $Al(OH)_3$ stimulation. As the gene targets were measured at mRNA level and the proteins induced by these measured genes were determined to be increased by proteomics-enabled mass spectrometry, it can be stated that the genes actually have been translated into

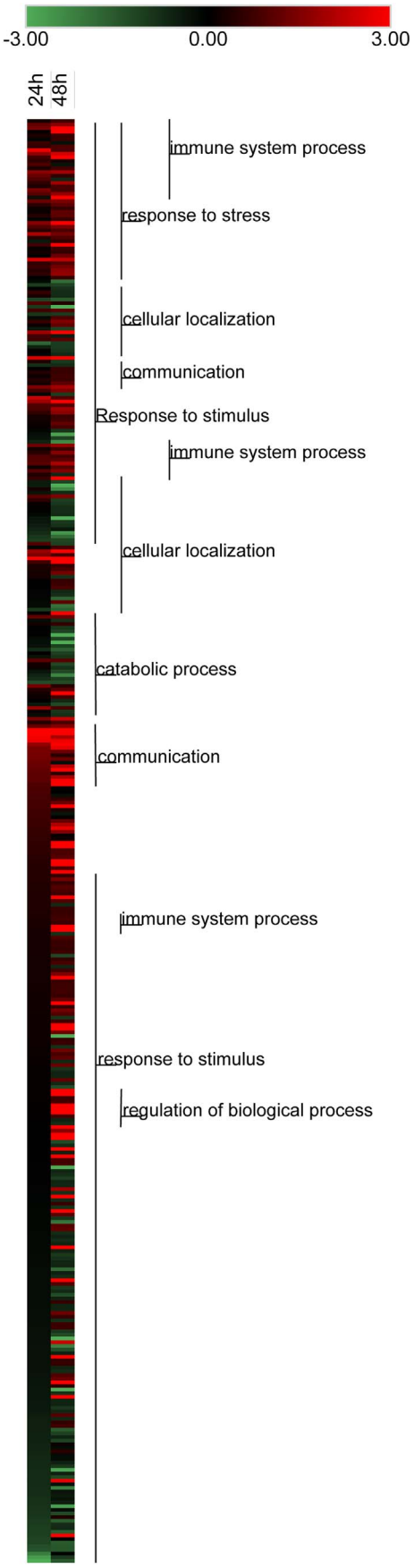

(caption on next page)

Fig. 2. Heatmap of all $Al(OH)_3$-regulated proteins in monocytes.
The heatmap represents the median of all upregulated (red) and downregulated (green) proteins from 3 biological replicates on a LOG2 scale after 24 and 48 h of $Al(OH)_3$ stimulation (10 μg/ml). Regulated proteins were at least altered by a factor 1.5 compared to the control in at least two out of three biological replicates. Enrichment analysis of GO biological processes was performed on the regulated proteins; depicted processes have FDRs < 0.05. The proteins were clustered by GO term as described in Supplementary S7.

proteins and subsequently induced downstream pathways; *e.g.* IFNβ induction was measured at the gene expression level and Mx1, Mx2 and IFIT3 were measured at protein level (Table 2 and Supplementary S7), these proteins are specifically induced by type I interferons [32, 33]. By combining the transcriptome and proteome analysis, pathways can be identified in more detail, despite the sometimes relative low coherence between protein and gene expression with respect to the same Uniprot entry. This might be related to the limited set of genes investigated, due to differences in kinetics or due to the fact that secreted proteins probably have not been identified in the cell lysates. By combining these techniques it is possible to analyze activated pathways, based on the identification of selected cytokines and downstream proteins.

One of the novel processes identified is the induction of IFNβ secretion resulting from $Al(OH)_3$ stimulation, most likely due to TLR2, TLR3 NOD like or other DAMP signaling. *IFNβ* gene expression was increased in $Al(OH)_3$-stimulated monocytes. Downstream of IFNβ, various proteins were induced: *e.g.* Mx1, Mx2 and IFIT3 were increased in $Al(OH)_3$-stimulated monocytes. These proteins can be induced by IFNβ *via STAT1*. Indeed, gene expression of *STAT1* was upregulated in $Al(OH)_3$-stimulated monocytes (Fig. 1). Upstream of IFNβ, *IRF7* gene expression was increased as was the expression of *IRF3* in two biological replicates. These inducers of type I interferon secretion can be activated *via* various pathways. Multiple of these inducers were identified and upregulated at the level of gene expression: *TICAM1*, *TRAF6*, *MyD88* and *IRAK1*. Upstream of these molecules, TLR signaling can be involved. In this data set, *TLR3* was upregulated at the level of gene expression. TLR2 was upregulated in two donors (Table 1). $Al(OH)_3$ is not a direct ligand for either of these pathways, however $Al(OH)_3$ causes the release of endogenous ligands by inducing cell death [13, 16, 19]. Indeed, markers of cell stress and cell death were identified in the

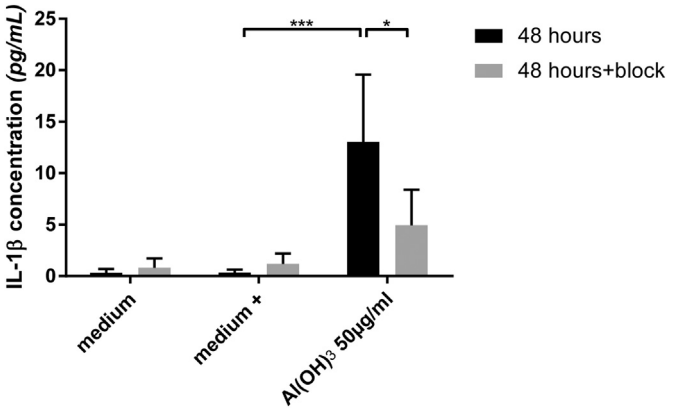

Fig. 4. IL-β levels in supernatants of THP-1 cell cultures upon $Al(OH)_3$ stimulation of THP-1 cells.
PMA-treated THP-1 cells were stimulated with 50 μg/ml $Al(OH)_3$ with or without the inflammasome blocker glybenclamide. IL-1β levels, measured after 48 h of stimulation, were compared to non-blocked $Al(OH)_3$-stimulated cells. Data are represented as the mean and the standard deviation of three independent experiments (biological replicates, each, with at least two technical replicates p-values < 0.05 are depicted as * and p-values < 0.005 are depicted as ***). Medium represents control cells, medium + represents medium with the PMA prime and 50 μg $Al(OH)_3$ represents the PMA-primed, $Al(OH)_3$-stimulated group.

protein dataset in this study (Fig. 3A, B, Supplementary S6–S9). These endogenous ligands can activate TLR3 and downstream signaling [44–46] and TLR2 directly or indirectly *via* TLR3 [51–54]. The activation of TLR3 results in recruitment of TICAM1 followed by the activation of IRF3/IRF7 leading to type I Interferon transcription. The activation of TLR2 can result in the formation of a complex with MyD88 and the internalization of this complex towards the endolysosome where this complex binds IRAK1. Subsequently, IRAK1 phosphorylates IRF3/IRF7, resulting in the transcription and secretion of type I interferons [48]. Many of the genes involved in these pathways were found to be upregulated as can be seen in Fig. 5. Since TLR2 was upregulated in two donors but downregulated in one donor, the pathway *via* TLR3 is

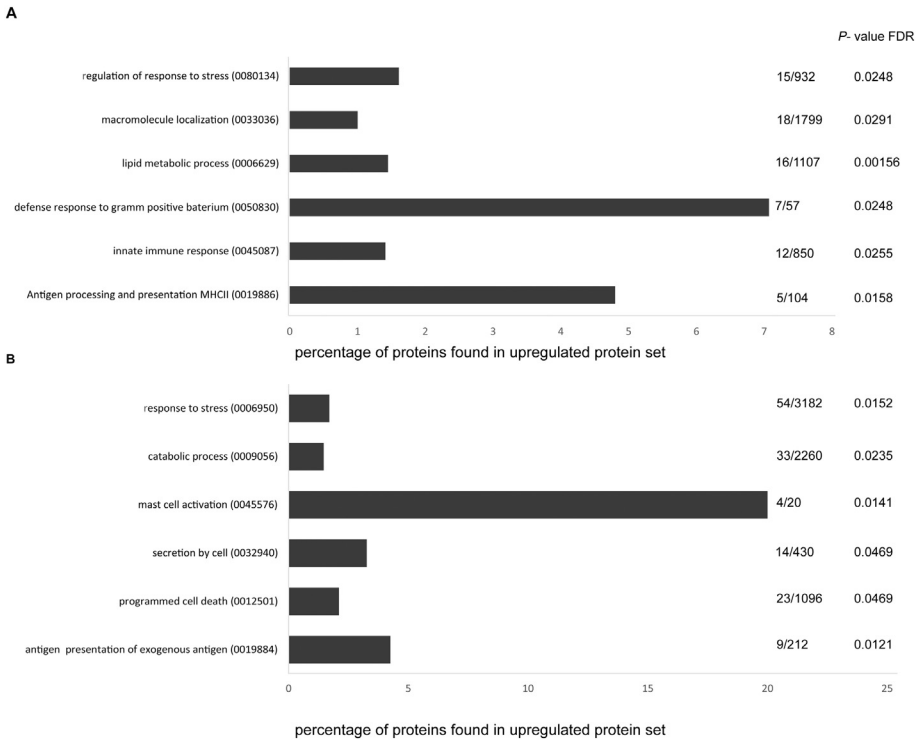

Fig. 3. Enriched GO biological process terms in the upregulated protein set after 24 and 48 h of $Al(OH)_3$stimulation of monocytes.
The GO terms are biological processes that are significantly overexpressed (p-values < 0.1) in the upregulated protein data set after 24 h of $Al(OH)_3$ stimulation (10 μg/ml) (3A) and 48 h (3B) from three biological replicates. The bars depict the percentage of upregulated proteins out of the total proteins in this GO term. The numbers display the ratios between upregulated proteins and total proteins in this GO term and the numbers between brackets are referring to the specified GO term.

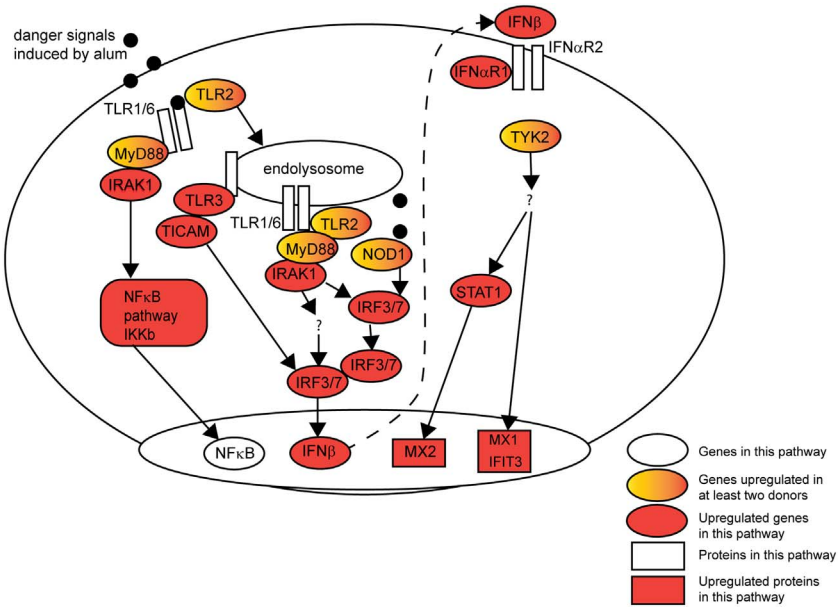

Fig. 5. Hypothetical pathways resulting in IFNβ secretion, potentially *via* TLR2/TLR3 and NOD1 pathways that become activated upon Al $(OH)_3$ stimulation of monocytes.
TLR2 and TLR3 can be activated by DAMPS, after which two pathways can be activated: one leading to the formation of NFκB and the second pathway leading to the formation of IFNβ and downstream proteins. NOD1 activation leads to the secretion of IFNβ. Genes are annotated in circles, proteins are annotated in boxes.

more likely to be involved in type I Interferon induction than the pathway *via* TLR2.

Detection of cytosolic DNA or other DAMPs is another possible cause of IFNβ induction [16]. Two of those DAMP sensors are NOD1 and DDX58 [19, 49, 50]. *NOD1* gene expression was found to be increased. Activation of NOD1 results in a similar pathway as the TLR2/TLR3 signaling pathway (Fig. 7). *DDX58* gene expression was upregulated in this data set, however, no further evidence of the activation of this pathway was identified. This is in agreement with the data from Marichal et al. describing that the DDX58-STING pathway might not be involved in the adjuvant effect of $Al(OH)_3$ [12, 19]. However, based on this data this pathway cannot be excluded. TLR8 and TLR9 are other potential DAMP sensors. Protein expression of TLR8 was downregulated and the gene expression of *TLR8* and *TLR9* was not increased in $Al(OH)_3$-stimulated monocytes, probably excluding TLR8 and TLR9 from a role in the adjuvant effect of $Al(OH)_3$. These results show that Al $(OH)_3$-induced DAMPS could be involved in the formation of IFNβ, most likely by activation TLR2 and/or TLR3 and by NOD1 signaling pathways, since many genes and proteins were upregulated in $Al(OH)_3$-stimulated cells that belong to these pathways. Other potential sensors for DNA in the cytoplasm signaling *via* the Caspase recruitment and activation domain (CARD) were not identified in the proteomics data, but cannot be excluded from being involved in Interferon secretion. It has been described that TLR signaling is not involved in the Ab response in $Al(OH)_3$-stimulated DCs [12, 15], however, a potential role for TLR signaling in the induction of interferons has been described earlier [16], as is the interaction with the inflammasome [55–57]. This data indicate that TLR signaling can be involved in the adjuvant effect of $Al(OH)_3$.

The induction and secretion of type I interferons can be related to processes described above, amongst others: differentiation away from a monocytic cell type, chemotaxis *via* the induction of CCL2, the increase of HLA class I and class II, activate complement and induce or inhibit the secretion of various cytokines as described previously [58–60]. This implies that type I interferons are crucial mediators of the innate immune response induced by $Al(OH)_3$. In addition, secretion of type I interferons (IFNβ) after $Al(OH)_3$ stimulation, might have several effects if the effects induce innate memory. Innate memory is the phenomenon of innate immune cells, like NK cells and macrophages, that are permanently changed after stimulation. Interferons play a role in inducing this innate memory [61]. First, type I interferons induced *via* TLR signaling are essential in the host response to virus. Second, they prime NK cells and macrophages [62, 63], of major importance for an early clearance of infections and the maturation of Th1 cells, which can be needed to induce memory [64, 65]. Third, type I interferons are essential for the survival of both $CD4^+$ and $CD8^+$ T cells [63], but most relevant for the immune response upon vaccination is the stimulation of local B cells by type I Interferons [66]. Therefore, IFNβ secretion can be important in the adjuvant effect of $Al(OH)_3$.

The other novel mechanism identified in this study is the increased activation of the antigen presentation pathway *via* HLA class I. It was recently described that activated monocytes have a fundamental role in antigen presentation to T cells in the lymph nodes and that antigen presenting monocytes can in fact cross present to HLA class I [24]. This study showed an upregulation of HLA class I molecules HLA-A and HLA-E, on both the level of gene expression and protein expression. Moreover, an increased protein expression of HM13 and an increased gene expression of *β2M* and *IFN*γ was observed, all related to antigen presentation *via* HLA class I [41, 67]. These results show that $Al(OH)_3$ increased the expression of HLA class I molecules on monocytes which leads to enhanced antigen presentation. Although $Al(OH)_3$ is capable of activating $CD8^+$ T cells, these T cells will likely not develop into mature cytotoxic T cells but rather into $CD8^+$ memory T cells [8, 13, 68–70]. Nevertheless, $Al(OH)_3$ is mainly considered an inducer of $CD4^+$ T cells [5, 13, 71]. HLA-E plays a role in the stimulation of NK cells. NK cells specifically recognize the HLA-*E*-peptide complex, which can inhibit and excite the response, depending if the peptide is self or foreign, such as a viral peptide [72, 73]. This is a useful process in inducing the immune response or preventing autoimmunity.

Besides increased expression of HLA class I molecules, an increased expression of components of the HLA class II pathway after $Al(OH)_3$ stimulation was observed, like Legumain, Cathepsins S, L, B and D. There is conflicting literature regarding the effect of $Al(OH)_3$ on HLA class II expression [5, 6, 74]. The increased expression of HLA class II molecules by $Al(OH)_3$ might be due to IFNγ signaling [41]. Indeed, in our study mRNA of *IFN*γ was increased. Moreover, protein expression of IFNγR1, and IFI30, a downstream molecule of the IFNγ signaling pathway, was increased. IFNγ-induced increase of HLA class II can be synergized by IL-3 and the IL-3R receptor, of which protein expression was increased [42]. The detection of several Cathepsins (S, L, D) and IFI30, which is required for antigen presentation *via* HLA class II, supports the hypothesis that $Al(OH)_3$ increases HLA class II antigen presentation by monocytes and that the increase of HLA class II molecules in monocytes might be due to the induction of IFNγ and subsequent signaling.

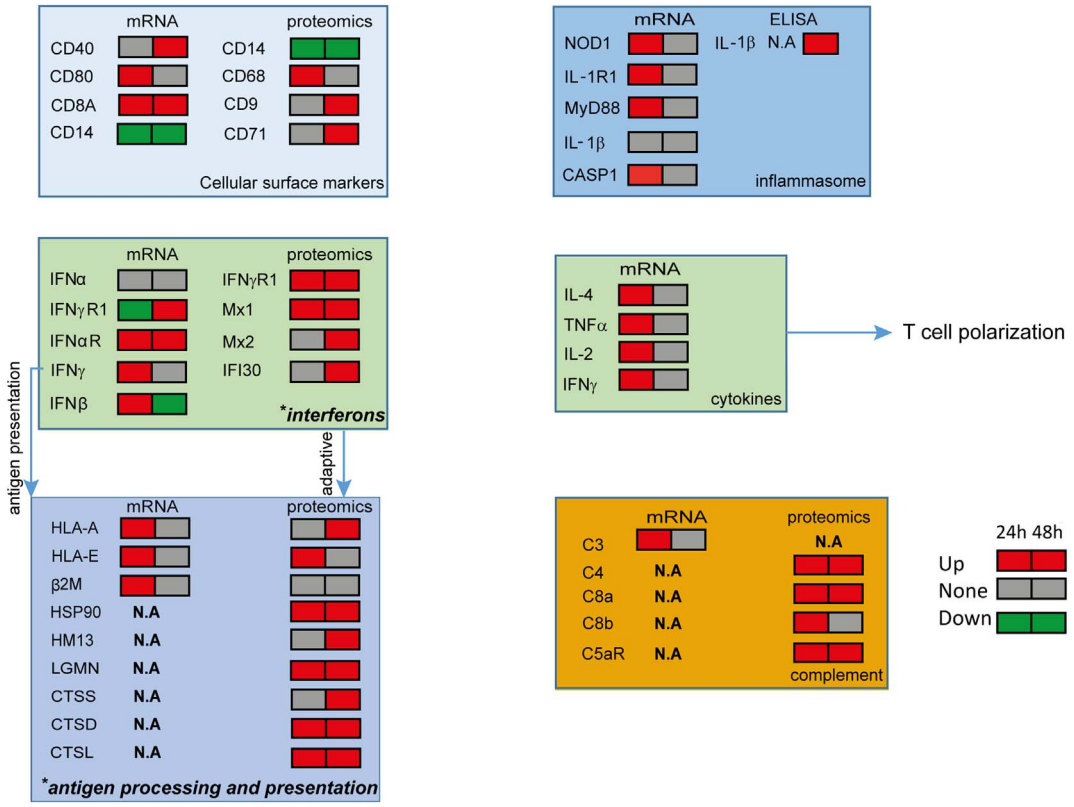

Fig. 6. Overview of the kinetics from the monocyte response towards $Al(OH)_3$ in combination with the analytical tool used.
The green blocks represent cytokines and related proteins. The light blue blocks represent the surface markers. The purple blocks represent the HLA-class I and class II antigen presentation pathways. The dark blue blocks represent the inflammasome activation. The orange blocks represent complement activation.

As described previously, $Al(OH)_3$ induced the downregulation of CD14 [6]. This finding indicates that $Al(OH)_3$-stimulated monocytes are starting to differentiate away from a monocytic cell type and that the cells become activated, which was confirmed by the increase of activation marker CD71 for monocytes. For the response to $Al(OH)_3$ it was expected that the response would be well measureable after 24 h, since the responses towards LPS could still be detected after 24 h; this time point was also based on the study of Ulanova et al. [75–77].

Induction of cytokines by an adjuvant is important in steering the immune response. $Al(OH)_3$ is described as an adjuvant that primes for a Th2 response by inducing IL-4 [5]. Indeed, our results show production of the Th2 polarizing cytokine *IL-4* by monocytes upon $Al(OH)_3$ stimulation. Presumably, the IL-4 response is dominant and may inhibit Th1 polarization In response to $Al(OH)_3$. However, innate IFNγ is associated with a Th1 response [36, 69]. A more Th1-related response to $Al(OH)_3$ was observed in multiple studies related to $Al(OH)_3$ [69]. IFNγ was secreted in IL-4 knockout mice [9] resulting in a more Th1-related response. IFNγ has more functions then solely being a Th1-associated cytokine. Thus, the polarization towards a Th2 type response occurs upon $Al(OH)_3$ stimulation despite the IFNγ produced.

One of the known mechanisms in the adjuvant activity of $Al(OH)_3$ besides preparing the innate immune system for antigen presentation and T cell activation, is the activation of the inflammasome leading to the secretion of IL-1β. This was confirmed in primary monocytes, by the increased gene expression of *NOD1*, *IL1R1* and a trend in *CASP1* and *MyD88*. In addition, a trend towards increased IL-1β secretion was observed in primary monocytes (2 donors) as was the reduction of IL-1β secretion when the inflammasome was blocked (1 donor). In PMA-primed THP-1 cells, an inflammasome inhibition experiment was performed that resulted in a reduced IL-1β secretion. PMA-primed THP-1 cells were used to further elucidate the inflammasome dependent origin of IL-β. THP-1 cells were used because, the levels of IL-1β detected in primary monocytes were low and THP-1 cells are a useful model since PMA priming causes the production of pro IL-1β and subsequent exposure to $Al(OH)_3$ can increase actual IL-1β, mimicking the two step activation required for inflammasome induction [78–80]. THP-1 cells are immortalized cells that differ in sensitivity form primary monocytes in response to stimuli such as LPS, due to differences in the cell surface marker expression of [81, 82]. However, the confirmation of the role of the inflammasome pathway in the IL-1β secretion in THP-1 cells suggests a similar involvement of the inflammasome in primary monocytes, since leads were also found in the primary monocyte data.

Complement activation is another mechanism described to be induced by $Al(OH)_3$ [18], either by $Al(OH)_3$ directly or by dying cells; genes and proteins related to the classical, alternative and lectin pathways were upregulated in this dataset [18]. In our study, transcriptome data revealed the upregulation of *C3* showing the initiation of the complement cascade, while at the level of the proteome C4, C5A and C8 were upregulated, representing the different complement pathways. These results show that combined use of transcriptomics and proteomics is valuable. At the transcriptome level, the initiation of the complement cascade was observed while with the proteome data the specific pathways were determined. The activation of complement pathways can be useful for bacterial lysis, and clearing apoptotic cells, which could prevent autoimmunity [83].

This study demonstrates that the response to $Al(OH)_3$ is very complex (Fig. 6), but also indicates that there might be considerable differences between *in vivo* and *in vitro* models. This might be caused by the use of a single cell type *in vitro versus* the availability of an intact, coherent immune system *in vivo*. Also, the species difference between cells from humans and mice might play a role. In mouse models, it was observed that $Al(OH)_3$ skews to a Th2 response [84]. In this study we indeed observed a polarization of the immune response towards a Th2 response, but in the presence of the Th1-associated gene IFNγ.

5. Conclusion

The immune response is a complex interplay of many molecules, residing in different tissues and cellular compartments. Hence, our model system, utilizing primary monocytes, does not include the coherent adaptive immune response upon $Al(OH)_3$ stimulus. Moreover, the present study did not include a particular antigen adsorbed to $Al(OH)_3$ which might also contribute to the innate immune response induced by $Al(OH)_3$.

Our systems biology-based approach revealed a detailed overview of the molecular mechanisms of $Al(OH)_3$ as an adjuvant for monocyte responsiveness (Fig. 6). Most important, the monocyte response to $Al(OH)_3$ is broad as illustrated by the induction of Th2-polarizing factors, the induction of type I and type II interferons and the upregulation of both HLA class I and HLA class II pathways, even in the absence of antigens. In this study, two new modes of action of $Al(OH)_3$ were elucidated, *i.e.* the upregulation of IFNγ in relation to HLA regulation and antigen presentation and the IFNβ secretion possibly as a result of TLR2, TLR3 or NOD1 activation. Finally, by combining complementary techniques, *e.g.* functional assays, transcriptome data and proteome data, it was possible to create a detailed overview of cellular processes in response to $Al(OH)_3$, which are important in the adjuvant effect of $Al(OH)_3$.

Supplementary data to this article can be found online at https://doi.org/10.1016/j.jprot.2017.12.021.

Transparency document

The Transparency document associated with this article can be found, in online version.

Acknowledgements

Sietske Kooijman is funded by a strategic research grant (SOR) of the Ministry of Health (IS200107). This work was also partly supported by the Proteins@Work, a program of the Netherlands Proteomics Centre financed by the Netherlands Organisation for Scientific Research (NWO) as part of the National Roadmap Large-scale Research Facilities of the Netherlands (project number 184.032.201).

We acknowledge Hilde Vrieling for performing the autofluorescent verification experiments for the flow cytometry data and for the THP-1 set up experiments.

References

[1] A.T. Glenny, C.G. Pope, H. Waddington, U. Wallace, Immunological notes. XVII–XXIV, J. Pathol. Bacteriol. 29 (1) (1926) 31–40.
[2] A.T. Glenny, G.A.H. Buttle, M.F. Stevens, Rate of disappearance of diphtheria toxoid injected into rabbits and guinea - pigs: Toxoid precipitated with alum, J. Pathol. Bacteriol. 34 (2) (1931) 267–275.
[3] L.B. Holt, Developments in Diptheria Prophylaxis, Heinemann, 1950.
[4] S.L. Hem, Elimination of aluminum adjuvants, Vaccine 20 (Suppl. 3) (2002) S40–3.
[5] M. Ulanova, A. Tarkowski, M. Hahn-Zoric, L.A. Hanson, The common vaccine adjuvant aluminum hydroxide up-regulates accessory properties of human monocytes via an interleukin-4-dependent mechanism, Infect. Immun. 69 (2) (2001) 1151–1159.
[6] A. Seubert, E. Monaci, M. Pizza, D.T. O'Hagan, A. Wack, The adjuvants aluminum hydroxide and MF59 induce monocyte and granulocyte chemoattractants and enhance monocyte differentiation toward dendritic cells, J. Immunol. 180 (8) (2008) 5402–5412.
[7] J.M. Brewer, M. Conacher, C.A. Hunter, M. Mohrs, F. Brombacher, J. Alexander, Aluminium hydroxide adjuvant initiates strong antigen-specific Th2 responses in the absence of IL-4- or IL-13-mediated signaling, J. Immunol. 163 (12) (1999) 6448–6454.
[8] A.S. McKee, M.W. Munks, M.K. MacLeod, C.J. Fleenor, N. Van Rooijen, J.W. Kappler, P. Marrack, Alum induces innate immune responses through macrophage and mast cell sensors, but these sensors are not required for alum to act as an adjuvant for specific immunity, J. Immunol. 183 (7) (2009) 4403–4414.
[9] J.M. Brewer, M. Conacher, A. Satoskar, H. Bluethmann, J. Alexander, In interleukin-4-deficient mice, alum not only generates T helper 1 responses equivalent to freund's complete adjuvant, but continues to induce T helper 2 cytokine production, Eur. J. Immunol. 26 (9) (1996) 2062–2066.
[10] A. Sokolovska, S.L. Hem, H. HogenEsch, Activation of dendritic cells and induction of CD4(+) T cell differentiation by aluminum-containing adjuvants, Vaccine 25 (23) (2007) 4575–4585.
[11] S. Calabro, M. Tortoli, B.C. Baudner, A. Pacitto, M. Cortese, D.T. O'Hagan, E. De Gregorio, A. Seubert, A. Wack, Vaccine adjuvants alum and MF59 induce rapid recruitment of neutrophils and monocytes that participate in antigen transport to draining lymph nodes, Vaccine 29 (9) (2011) 1812–1823.
[12] P. He, Y. Zou, Z. Hu, Advances in aluminum hydroxide-based adjuvant research and its mechanism, Hum. Vaccin. Immunother 11 (2) (2015) 477–488.
[13] M. Kool, T. Soullie, M. van Nimwegen, M.A. Willart, F. Muskens, S. Jung, H.C. Hoogsteden, H. Hammad, B.N. Lambrecht, Alum adjuvant boosts adaptive immunity by inducing uric acid and activating inflammatory dendritic cells, J. Exp. Med. 205 (4) (2008) 869–882.
[14] H. Li, S.B. Willingham, J.P. Ting, F. Re, Cutting edge: inflammasome activation by alum and alum's adjuvant effect are mediated by NLRP3, J. Immunol. 181 (1) (2008) 17–21.
[15] M. Kool, V. Petrilli, T. De Smedt, A. Rolaz, H. Hammad, M. van Nimwegen, I.M. Bergen, R. Castillo, B.N. Lambrecht, J. Tschopp, Cutting edge: alum adjuvant stimulates inflammatory dendritic cells through activation of the NALP3 inflammasome, J. Immunol. 181 (6) (2008) 3755–3759.
[16] M. Kool, K. Fierens, B.N. Lambrecht, Alum adjuvant: some of the tricks of the oldest adjuvant, J. Med. Microbiol. 61 (Pt 7) (2012) 927–934.
[17] L. Franchi, G. Nunez, The Nlrp3 inflammasome is critical for aluminium hydroxide-mediated IL-1beta secretion but dispensable for adjuvant activity, Eur. J. Immunol. 38 (8) (2008) 2085–2089.
[18] E. Guven, K. Duus, I. Laursen, P. Hojrup, G. Houen, Aluminum hydroxide adjuvant differentially activates the three complement pathways with major involvement of the alternative pathway, PLoS One 8 (9) (2013) e74445.
[19] T. Marichal, K. Ohata, D. Bedoret, C. Mesnil, C. Sabatel, K. Kobiyama, P. Lekeux, C. Coban, S. Akira, K.J. Ishii, F. Bureau, C.J. Desmet, DNA released from dying host cells mediates aluminum adjuvant activity, Nat. Med. 17 (8) (2011) 996–1002.
[20] A.S. McKee, M.A. Burchill, M.W. Munks, L. Jin, J.W. Kappler, R.S. Friedman, J. Jacobelli, P. Marrack, Host DNA released in response to aluminum adjuvant enhances MHC class II-mediated antigen presentation and prolongs CD4 T-cell interactions with dendritic cells, Proc. Natl. Acad. Sci. U. S. A. 110 (12) (2013) E1122–31.
[21] S.C. Eisenbarth, O.R. Colegio, W. O'Connor, F.S. Sutterwala, R.A. Flavell, Crucial role for the Nalp3 inflammasome in the immunostimulatory properties of aluminium adjuvants, Nature 453 (7198) (2008) 1122–1126.
[22] M. Rossi, J.W. Young, Human dendritic cells: potent antigen-presenting cells at the crossroads of innate and adaptive immunity, J. Immunol. 175 (3) (2005) 1373–1381.
[23] A. Rivera, M.C. Siracusa, G.S. Yap, W.C. Gause, Innate cell communication kick-starts pathogen-specific immunity, Nat. Immunol. 17 (4) (2016) 356–363.
[24] C.V. Jakubzick, G.J. Randolph, P.M. Henson, Monocyte differentiation and antigen-presenting functions, Nat. Rev. Immunol. 17 (6) (2017) 349–362.
[25] E. Elkord, P.E. Williams, H. Kynaston, A.W. Rowbottom, Human monocyte isolation methods influence cytokine production from in vitro generated dendritic cells, Immunology 114 (2) (2005) 204–212.
[26] H.D. Meiring, E.C. Soethout, M.C. Poelen, D. Mooibroek, R. Hoogerbrugge, H. Timmermans, C.J. Boog, A.J. Heck, A.P. de Jong, C.A. van Els, Stable isotope tagging of epitopes: a highly selective strategy for the identification of major histocompatibility complex class I-associated peptides induced upon viral infection, Mol. Cell. Proteomics 5 (5) (2006) 902–913.
[27] H.D. Meiring, E. van der Heeft, G.J. ten Hove, A.P.J.M. de Jong, Nanoscale LC-MS(n): technical design and applications to peptide and protein analysis, J. Sep. Sci. 25 (9) (2002) 557–568.
[28] L. Moruz, P. Pichler, T. Stranzl, K. Mechtler, L. Kall, Optimized nonlinear gradients for reversed-phase liquid chromatography in shotgun proteomics, Anal. Chem. 85 (16) (2013) 7777–7785.
[29] D. Szklarczyk, A. Franceschini, S. Wyder, K. Forslund, D. Heller, J. Huerta-Cepas, M. Simonovic, A. Roth, A. Santos, K.P. Tsafou, M. Kuhn, P. Bork, L.J. Jensen, C. von Mering, STRING v10: protein-protein interaction networks, integrated over the tree of life, Nucleic Acids Res. 43 (Database issue) (2015) D447–52.
[30] J.A. Vizcaino, A. Csordas, N. Del-Toro, J.A. Dianes, J. Griss, I. Lavidas, G. Mayer, Y. Perez-Riverol, F. Reisinger, T. Ternent, Q.W. Xu, R. Wang, H. Hermjakob, 2016 update of the PRIDE database and its related tools, Nucleic Acids Res. 44 (22) (2016) 11033.
[31] S.D. Wright, R.A. Ramos, P.S. Tobias, R.J. Ulevitch, J.C. Mathison, CD14, a receptor for complexes of lipopolysaccharide (LPS) and LPS binding protein, Science 249 (4975) (1990) 1431–1433.
[32] D. Holzinger, C. Jorns, S. Stertz, S. Boisson-Dupuis, R. Thimme, M. Weidmann, J.L. Casanova, O. Haller, G. Kochs, Induction of MxA gene expression by influenza A virus requires type I or type III interferon signaling, J. Virol. 81 (14) (2007) 7776–7785.
[33] L.M. Pletneva, O. Haller, D.D. Porter, G.A. Prince, J.C. Blanco, Induction of type I interferons and interferon-inducible Mx genes during respiratory syncytial virus infection and reinfection in cotton rats, J. Gen. Virol. 89 (Pt 1) (2008) 261–270.
[34] A. Simon, J. Fah, O. Haller, P. Staeheli, Interferon-regulated Mx genes are not responsive to interleukin-1, tumor necrosis factor, and other cytokines, J. Virol. 65 (2) (1991) 968–971.
[35] N. Dubois Cauwelaert, A.L. Desbien, T.E. Hudson, S.O. Pine, S.G. Reed, R.N. Coler, M.T. Orr, The TLR4 agonist vaccine adjuvant, GLA-SE, requires canonical and atypical mechanisms of action for TH1 induction, PLoS One 11 (1) (2016) e0146372.
[36] A. O'Garra, Cytokines induce the development of functionally heterogeneous T

helper cell subsets, Immunity 8 (3) (1998) 275–283.
[37] A.N. Antoniou, S.L. Blackwood, D. Mazzeo, C. Watts, Control of antigen presentation by a single protease cleavage site, Immunity 12 (4) (2000) 391–398.
[38] K. Wolk, G. Grutz, K. Witte, H.D. Volk, R. Sabat, The expression of legumain, an asparaginyl endopeptidase that controls antigen processing, is reduced in endotoxin-tolerant monocytes, Genes Immun. 6 (5) (2005) 452–456.
[39] B. Manoury, E.W. Hewitt, N. Morrice, P.M. Dando, A.J. Barrett, C. Watts, An asparaginyl endopeptidase processes a microbial antigen for class II MHC presentation, Nature 396 (6712) (1998) 695–699.
[40] C. Tulone, A.M. Sponaas, E.A. Raiber, A.B. Tabor, J. Langhorne, B.M. Chain, Differential requirement for cathepsin D for processing of the full length and C-terminal fragment of the malaria antigen MSP1, PLoS One 6 (10) (2011) e24886.
[41] P. Keskinen, T. Ronni, S. Matikainen, A. Lehtonen, I. Julkunen, Regulation of HLA class I and II expression by interferons and influenza A virus in human peripheral blood mononuclear cells, Immunology 91 (3) (1997) 421–429.
[42] E.I. Korpelainen, J.R. Gamble, W.B. Smith, M. Dottore, M.A. Vadas, A.F. Lopez, Interferon-gamma upregulates interleukin-3 (IL-3) receptor expression in human endothelial cells and synergizes with IL-3 in stimulating major histocompatibility complex class II expression and cytokine production, Blood 86 (1) (1995) 176–182.
[43] K. Honda, T. Taniguchi, IRFs: master regulators of signalling by Toll-like receptors and cytosolic pattern-recognition receptors, Nat. Rev. Immunol. 6 (9) (2006) 644–658.
[44] K. Kariko, H. Ni, J. Capodici, M. Lamphier, D. Weissman, mRNA is an endogenous ligand for Toll-like receptor 3, J. Biol. Chem. 279 (13) (2004) 12542–12550.
[45] K.A. Cavassani, M. Ishii, H. Wen, M.A. Schaller, P.M. Lincoln, N.W. Lukacs, C.M. Hogaboam, S.L. Kunkel, TLR3 is an endogenous sensor of tissue necrosis during acute inflammatory events, J. Exp. Med. 205 (11) (2008) 2609–2621.
[46] X. Zhang, D.M. Mosser, Macrophage activation by endogenous danger signals, J. Pathol. 214 (2) (2008) 161–178.
[47] K.J. Ishii, S. Koyama, A. Nakagawa, C. Coban, S. Akira, Host innate immune receptors and beyond: making sense of microbial infections, Cell Host Microbe 3 (6) (2008) 352–363.
[48] N. Dietrich, S. Lienenklaus, S. Weiss, N.O. Gekara, Murine toll-like receptor 2 activation induces type I interferon responses from endolysosomal compartments, PLoS One 5 (4) (2010) e10250.
[49] H. Antosz, M. Osiak, NOD1 and NOD2 receptors: integral members of the innate and adaptive immunity system, Acta Biochim. Pol. 60 (3) (2013) 351–360.
[50] A.A. Shigeoka, A. Kambo, J.C. Mathison, A.J. King, W.F. Hall, J. da Silva Correia, R.J. Ulevitch, D.B. McKay, Nod1 and nod2 are expressed in human and murine renal tubular epithelial cells and participate in renal ischemia reperfusion injury, J. Immunol. 184 (5) (2010) 2297–2304.
[51] J. Lichtnekert, V. Vielhauer, D. Zecher, O.P. Kulkarni, S. Clauss, S. Segerer, V. Hornung, T.N. Mayadas, B. Beutler, S. Akira, H.J. Anders, Trif is not required for immune complex glomerulonephritis: dying cells activate mesangial cells via Tlr2/Myd88 rather than Tlr3/Trif, Am. J. Physiol. Ren. Physiol. 296 (4) (2009) F867–74.
[52] K. Mori, M. Yanagita, S. Hasegawa, M. Kubota, M. Yamashita, S. Yamada, M. Kitamura, S. Murakami, Necrosis-induced TLR3 activation promotes TLR2 expression in gingival cells, J. Dent. Res. 94 (8) (2015) 1149–1157.
[53] K.A. Scheibner, M.A. Lutz, S. Boodoo, M.J. Fenton, J.D. Powell, M.R. Horton, Hyaluronan fragments act as an endogenous danger signal by engaging TLR2, J. Immunol. 177 (2) (2006) 1272–1281.
[54] L. Yu, L. Wang, S. Chen, Endogenous toll-like receptor ligands and their biological significance, J. Cell. Mol. Med. 14 (11) (2010) 2592–2603.
[55] M.V. Suresh, B. Thomas, D. Machado-Aranda, V.A. Dolgachev, S. Kumar Ramakrishnan, N. Talarico, K. Cavassani, M.A. Sherman, M.R. Hemmila, S.L. Kunkel, N.G. Walter, C.M. Hogaboam, K. Raghavendran, Double-stranded RNA interacts with Toll-like receptor 3 in driving the acute inflammatory response following lung contusion, Crit. Care Med. 44 (11) (2016) e1054–e1066.
[56] C.E. Becker, L.A. O'Neill, Inflammasomes in inflammatory disorders: the role of TLRs and their interactions with NLRs, Semin. Immunopathol. 29 (3) (2007) 239–248.
[57] E.K. Grishman, P.C. White, R.C. Savani, Toll-like receptors, the NLRP3 inflammasome, and interleukin-1beta in the development and progression of type 1 diabetes, Pediatr. Res. 71 (6) (2012) 626–632.
[58] I. Rauch, M. Muller, T. Decker, The regulation of inflammation by interferons and their STATs, JAKSTAT 2 (1) (2013) e23820.
[59] R. Asokan, J. Hua, K.A. Young, H.J. Gould, J.P. Hannan, D.M. Kraus, G. Szakonyi, G.J. Grundy, X.S. Chen, M.K. Crow, V.M. Holers, Characterization of human complement receptor type 2 (CR2/CD21) as a receptor for IFN-alpha: a potential role in systemic lupus erythematosus, J. Immunol. 177 (1) (2006) 383–394.
[60] S. Hervas-Stubbs, J.L. Perez-Gracia, A. Rouzaut, M.F. Sanmamed, A. Le Bon, I. Melero, Direct effects of type I interferons on cells of the immune system, Clin. Cancer Res. 17 (9) (2011) 2619–2627.
[61] M.G. Netea, L.A. Joosten, E. Latz, K.H. Mills, G. Natoli, H.G. Stunnenberg, L.A. O'Neill, R.J. Xavier, Trained immunity: a program of innate immune memory in health and disease, Science 352 (6284) (2016) aaf1098.
[62] E. Szomolanyi-Tsuda, X. Liang, R.M. Welsh, E.A. Kurt-Jones, R.W. Finberg, Role for TLR2 in NK cell-mediated control of murine cytomegalovirus in vivo, J. Virol. 80 (9) (2006) 4286–4291.
[63] F.P. Siegal, N. Kadowaki, M. Shodell, P.A. Fitzgerald-Bocarsly, K. Shah, S. Ho, S. Antonenko, Y.J. Liu, The nature of the principal type 1 interferon-producing cells in human blood, Science 284 (5421) (1999) 1835–1837.
[64] O. Joffre, M.A. Nolte, R. Sporri, C. Reis e Sousa, Inflammatory signals in dendritic cell activation and the induction of adaptive immunity, Immunol. Rev. 227 (1) (2009) 234–247.
[65] M.P. Longhi, C. Trumpfheller, J. Idoyaga, M. Caskey, I. Matos, C. Kluger, A.M. Salazar, M. Colonna, R.M. Steinman, Dendritic cells require a systemic type I interferon response to mature and induce CD4+ Th1 immunity with poly IC as adjuvant, J. Exp. Med. 206 (7) (2009) 1589–1602.
[66] E.S. Coro, W.L. Chang, N. Baumgarth, Type I IFN receptor signals directly stimulate local B cells early following influenza virus infection, J. Immunol. 176 (7) (2006) 4343–4351.
[67] M.K. Lemberg, F.A. Bland, A. Weihofen, V.M. Braud, B. Martoglio, Intramembrane proteolysis of signal peptides: an essential step in the generation of HLA-E epitopes, J. Immunol. 167 (11) (2001) 6441–6446.
[68] S.B. Dillon, S.G. Demuth, M.A. Schneider, C.B. Weston, C.S. Jones, J.F. Young, M. Scott, P.K. Bhatnaghar, S. LoCastro, N. Hanna, Induction of protective class I MHC-restricted CTL in mice by a recombinant influenza vaccine in aluminium hydroxide adjuvant, Vaccine 10 (5) (1992) 309–318.
[69] H. Hogenesch, Mechanism of immunopotentiation and safety of aluminum adjuvants, Front. Immunol. 3 (2012) 406.
[70] M.K. MacLeod, A.S. McKee, A. David, J. Wang, R. Mason, J.W. Kappler, P. Marrack, Vaccine adjuvants aluminum and monophosphoryl lipid A provide distinct signals to generate protective cytotoxic memory CD8 T cells, Proc. Natl. Acad. Sci. U. S. A. 108 (19) (2011) 7914–7919.
[71] E.B. Lindblad, Aluminium compounds for use in vaccines, Immunol. Cell Biol. 82 (5) (2004) 497–505.
[72] V.M. Braud, D.S. Allan, C.A. O'Callaghan, K. Soderstrom, A. D'Andrea, G.S. Ogg, S. Lazetic, N.T. Young, J.I. Bell, J.H. Phillips, L.L. Lanier, A.J. McMichael, HLA-E binds to natural killer cell receptors CD94/NKG2A, B and C, Nature 391 (6669) (1998) 795–799.
[73] A.G. Brooks, F. Borrego, P.E. Posch, A. Patamawenu, C.J. Scorzelli, M. Ulbrecht, E.H. Weiss, J.E. Coligan, Specific recognition of HLA-E, but not classical, HLA class I molecules by soluble CD94/NKG2A and NK cells, J. Immunol. 162 (1) (1999) 305–313.
[74] H. Sun, K.G. Pollock, J.M. Brewer, Analysis of the role of vaccine adjuvants in modulating dendritic cell activation and antigen presentation in vitro, Vaccine 21 (9–10) (2003) 849–855.
[75] Y. Zheng, C.N. Manzotti, M. Liu, F. Burke, K.I. Mead, D.M. Sansom, CD86 and CD80 differentially modulate the suppressive function of human regulatory T cells, J. Immunol. 172 (5) (2004) 2778–2784.
[76] T.J. Lang, P. Nguyen, R. Peach, W.C. Gause, C.S. Via, In vivo CD86 blockade inhibits CD4+ T cell activation, whereas CD80 blockade potentiates CD8+ T cell activation and CTL effector function, J. Immunol. 168 (8) (2002) 3786–3792.
[77] D. Odobasic, M.T. Leech, J.R. Xue, S.R. Holdsworth, Distinct in vivo roles of CD80 and CD86 in the effector T-cell responses inducing antigen-induced arthritis, Immunology 124 (4) (2008) 503–513.
[78] H. Guo, J.B. Callaway, J.P. Ting, Inflammasomes: mechanism of action, role in disease, and therapeutics, Nat. Med. 21 (7) (2015) 677–687.
[79] M.G. Ghonime, O.R. Shamaa, S. Das, R.A. Eldomany, T. Fernandes-Alnemri, E.S. Alnemri, M.A. Gavrilin, M.D. Wewers, Inflammasome priming by lipopolysaccharide is dependent upon ERK signaling and proteasome function, J. Immunol. 192 (8) (2014) 3881–3888.
[80] S.P. Cullen, C.J. Kearney, D.M. Clancy, S.J. Martin, Diverse activators of the NLRP3 inflammasome promote IL-1beta secretion by triggering necrosis, Cell Rep. 11 (10) (2015) 1535–1548.
[81] W. Chanput, J.J. Mes, H.J. Wichers, THP-1 cell line: an in vitro cell model for immune modulation approach, Int. Immunopharmacol. 23 (1) (2014) 37–45.
[82] H. Bosshart, M. Heinzelmann, THP-1 cells as a model for human monocytes, Ann. Transl. Med. 4 (21) (2016) 438.
[83] Z. Fishelson, G. Attali, D. Mevorach, Complement and apoptosis, Mol. Immunol. 38 (2–3) (2001) 207–219.
[84] F. Mosca, E. Tritto, A. Muzzi, E. Monaci, F. Bagnoli, C. Iavarone, D. O'Hagan, R. Rappuoli, E. De Gregorio, Molecular and cellular signatures of human vaccine adjuvants, Proc. Natl. Acad. Sci. U. S. A. 105 (30) (2008) 10501–10506.